Available online at www.sciencedirect.com
SCIENCE DIRECT®
International Journal of Heat and Mass Transfer 47 (2004) 1515–1524
International Journal of HEAT and MASS TRANSFER
www.elsevier.com/locate/ijhmt

# Chaos in nucleate boiling—nonlinear analysis and modelling

R. Mosdorf [a,*], M. Shoji [b,1]

[a] Faculty of Computer Science, Bialystok University of Technology, ul. Wiejska 45, Bialystok 15-351, Poland
[b] Department of Mechanical Engineering, The University of Tokyo, 7-3-1Hongo, Bunkyo-ku, Tokyo 113-8656, Japan

**Abstract**

The artificial surfaces are applied to study the pool boiling features, including the surface temperature fluctuation and nucleation sites interaction. The nonlinear analysis of temperature fluctuation has been carried out. Under the single nucleation site the low dimensional deterministic chaos has been observed. It has been found that the thermal interaction between two nucleation sites decreases and the hydrodynamic interaction increases the frequency of bubble departure. It has been also found out that hydrodynamic interaction makes that the process of bubbles departure becomes more predictable. To explain the mechanism of deterministic chaos appearance the simple model of heat transfer under the nucleation sites has been presented. The obtained results of simulations show that the nonlinearity introduced to heat transfer as a result of changing in time the heat flux absorbed by bubbles leads to chaotic changes of heating surface temperature at nucleation site. The model has been used to analyse the behavior of thermal interaction between nucleation sites with chaotically departing bubbles. The results obtained from simulation explain experimental results.


*Keywords:* Pool boiling; Artificial surface; Boiling chaos; Nucleation site interaction

## 1. Introduction

Despite of the extensive study of boiling during the past over fifty years, the underlying mechanisms of nucleate boiling are still far from being fully understood due to the extreme complexity of the phenomena. In boiling phenomena, not a small number of sub-processes may involve and their mutual interactions are complicated and of nonlinear nature. Among the sub-processes, the most important one may be the nucleation site problem [1]. In this case two behaviors play important role in understanding the nucleation site problem. The first one is connected with mutual interaction between the bubbles and heating surface. The second one is connected with interaction of neighbouring nucleation site. Interacting bubbles create a complex dynamical system which includes such processes as: heat transfer (in liquid, between bubble and heating surface), phase changes, different kind of bubbles coalescence, contact behaviors and liquid flow around the bubble. All these processes are mutually connected, therefore the complexity level of system is very high.

The structure of actual heater surface is very complicated and there exists many nucleation cavities with various shapes and sizes. Moreover, we have unfortunately no useful measure to rigorously capture such surface property. This is the main reason why we have had limited success in mechanistic modelling of boiling. So the one possible approach to solve this problem is to simplify the boiling surface as far as possible in order to clarify the underlying mechanisms. In recent years, the technique of micromachining has markedly advanced in accordance with the advancement of electronic devices and microtechnologies and it is now possible to produce a smooth surface with only prescribed cavities. At the same time, it may also be useful to apply together

* Corresponding author. Tel.: +48-85-7422-041; fax: +48-85-7422-393.
*E-mail addresses:* mosdorf@ii.pb.bialystok.pl (R. Mosdorf), shoji@photon.t.u-tokyo.ac.jp (M. Shoji).
[1] Tel.: +81-3-5841-6406; fax: +81-3-5800-6987.

0017-9310/$ - see front matter © 2003 Elsevier Ltd. All rights reserved.
doi:10.1016/j.ijheatmasstransfer.2003.09.022

**Nomenclature**

| | |
|---|---|
| $A$ | coefficient equal to $1/Fo$ |
| $a, b, d$ | constant |
| $c$ | specific heat capacity |
| $C$ | correlation coefficient |
| $D$ | dimension |
| $d$ | distance in phase space |
| $f$ | function |
| $Fo$ | Fourier number |
| $L$ | largest Lyapunov exponent |
| $N$ | number of points |
| $q$ | heat flux |
| $T$ | temperature |
| $t$ | time |
| $X$ | experimental data |

*Greek symbols*

| | |
|---|---|
| $\Theta$ | Heaviside's step function |
| $\delta$ | size of element of heating surface |
| $\lambda$ | thermal conductivity |
| $\sigma$ | standard deviation |
| $\rho$ | density |

*Subscripts*

| | |
|---|---|
| 1,2 | number of coefficient |
| c | crossing point |
| F, B, L, R | neighbouring elements |
| $i$ | considered element, number of reference points |
| $j$ | number of points |
| $q$ | parameter |

*Superscript*

| | |
|---|---|
| $k$ | iteration number |

recently advanced nonlinear chaos dynamics for the data analysis to make clear the underlying complex dynamics.

By applying the artificial boiling surfaces, some researchers have already investigated the boiling heat transfer characteristics, the bubble behaviors and the surface temperature fluctuation. Qiu and Dhir [2] studied the growth and detachment mechanisms of a single bubble on a heated silicon surface with an artificial cavity of 10 μm in diameter and 100 μm in depth. Bubble growth time, bubble size and shape were measured from nucleation to departure under sub-cooled and saturation conditions. Takagi and Shoji [9], Ellepola and Kenning [10] and Kenning and Yan [15] also analysed the nonlinear dynamic of bubble growth in artificial cavities. On the other hand, the relation between the bubble behaviors and the cavity spacing, $S/D$, has been studied experimentally by Chekanov [3], Calka and Judd [4], Gjerkeš and Golobic [5]. Several authors have studied the heat transfer characteristics of the artificial boiling surfaces with multiple cavities aiming applications to the cooling of highly integrated electronic devices [6,7]. Recently, by employing twin cavities, Zhang and Shoji [8] have investigated the mechanism of nucleation sites interaction.

In the paper the nonlinear analysis of temperature fluctuation under the artificial nucleation sites has been carried out. The simple model of generation of chaotic changes of heating surface temperature has been presented. The model has been used to explain the mechanism of deterministic chaos generation and to investigate the nature of thermal interaction between the nucleation sites.

## 2. Experimental setup

A 15 mm × 15 mm and 200 μm thick silicon disk with artificial nucleation sites was set as a test boiling surface inside the chamber filled with distilled water. Schematic view of the whole experimental setup is shown in Fig. 1. In the experiment, vicinity of the manufactured cavity was heated by Nd–YAG laser irradiation (wavelength: 1064 nm) from the bottom side of the test disk. The size of laser spot was 12 mm in diameter. The bottom surface of the disk was black oxide finished in order to improve

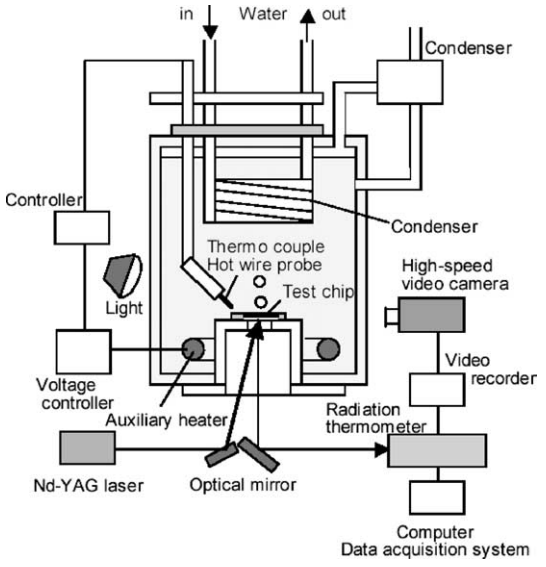


Fig. 1. Experimental apparatus.

absorptivity of the input laser and emissivity from the surface. Temperature fluctuation just under the artificial cavity were recorded by radiation thermometer with spatial resolution of 120 μm, temperature resolution of 0.08 K and time resolution of 3.0 ms. The corresponding bubbling status was recorded by high-speed video camera with the rate of 1297 frames/s. In this way, it was possible to measure temperature time series of cavity vicinity without any physical contact to the disk surface. The power of Nd–YAG laser was controlled to vary the heat input to the disk surface and was monitored by photo detector throughout the experiment. Working fluid was distilled water at atmospheric pressure under saturated pool boiling condition. Acrylic fence was set inside the chamber to avoid effect of bubbling from auxiliary heater, which was activated during the experiment to maintain saturated boiling condition.

## 3. Single nucleation site

The identification of mechanism of nucleation sites interaction is possible after understanding the dynamic of bubbles interaction with the heating surface. As it has been shown by Shoji et al. [18] we can distinguish at least two mechanisms of bubbles interaction with heating surface. The first one is connected with direct heat transfer between the subsequent bubbles and heating surface under the nucleation site. The other one is connected with heat transfer between the heating surface around the nucleation site and liquid flow induced by subsequent departing bubbles. The first mechanism is characterized by low number of freedom degree, therefore it is useful for understanding the changes of dynamic of bubbles departure caused by nucleation sites interaction.

For analysing the behavior of single nucleation site a silicon plate with cylindrical nucleation site was applied as a test surface. The nucleation site of 10 μm in diameter and 80 μm in depth was used because in this kind of nucleation site the low dimensional dynamic of temperature changes is observed [18]. In the experiment the heat supplied to the heating surface was enough to obtain such a regime of bubbles departure in which the bubbles were departing from the nucleation site without waiting time between the subsequent bubbles. In this case after the bubble departure the new bubble starts to grow immediately. In considered case the temperature changes under the nucleation site are directly connected with changes in time of the heat flux absorbed by subsequent bubbles. A convection process does not influence on heat transfer at nucleation site. The example of bubble growth and its departure has been shown in Fig. 2 where subsequent frames of video taken in time interval equal to 1/1297 s have been shown. In Fig. 2a it has been shown the end phase of bubble departure and in Fig. 2b the initial phase of a rapid bubble growth.

The example of temperature changes at the nucleation site has been shown in Fig. 3.

The dynamic of temperature changes at the nucleation site is complex, it depends on temperature of heating surface, the shape of nucleation site [18] and conditions around the bubbles. The example of 3D attractor reconstruction from temperature fluctuation at the single nucleation site has been shown in Fig. 4. The structure of attractors suggests that subsequent departing bubbles create some kind of chaotic thermal oscillator. The temperature changes create the triangle shape of attractor trajectories in phase space. During the bubble departure the temperature at nucleation site oscillates. The temperature increases when the heat supplied to heating surface is greater than the heat absorbed

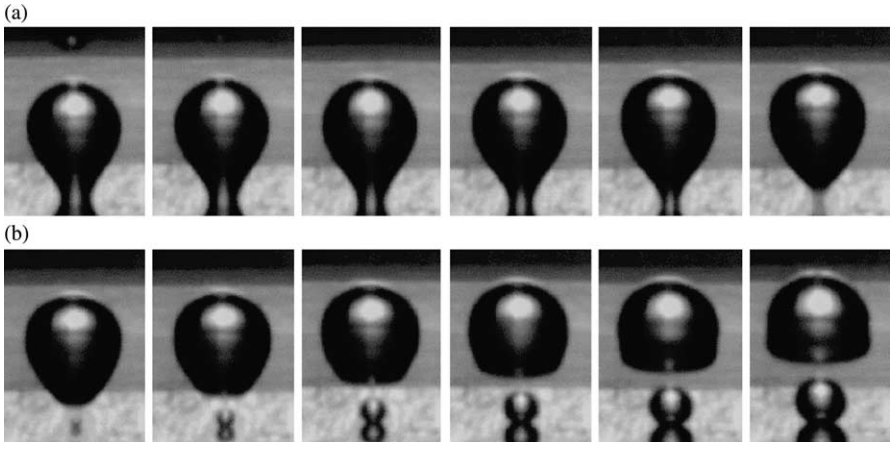


Fig. 2. Subsequent stages of bubble growth. The time between the pictures is equal to 1/1297 s. (a) rapid bubble growth, (b) bubble departure.

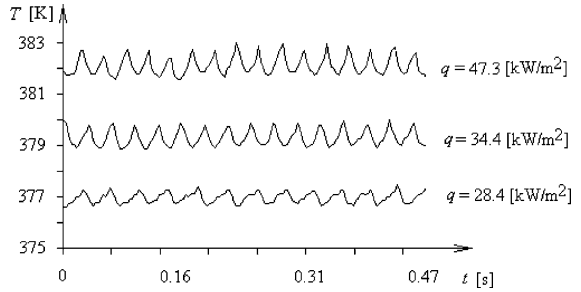


Fig. 3. Temperature changes under the cavity in three value of $q$.

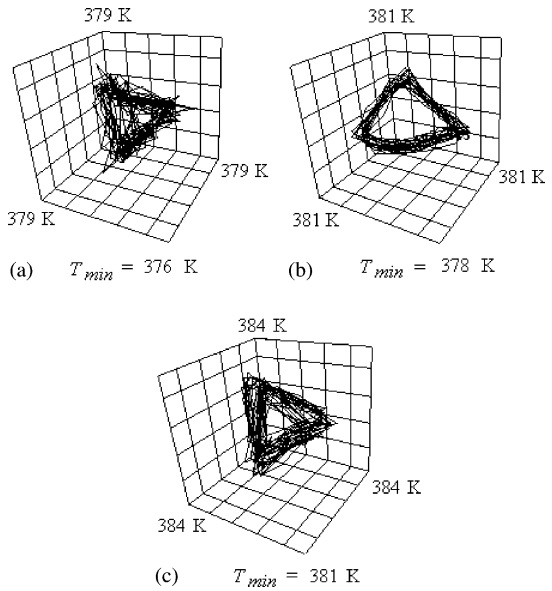


Fig. 4. The 3D attractor reconstruction from the temperature fluctuation under the single cavity. (a) $q = 28.4$ kW/m$^2$, time delay 0.026 s, (b) $q = 34.4$ kW/m$^2$, time delay 0.023 s, (c) $q = 47.3$ kW/m$^2$, time delay 0.023 s.

by boiling liquid and when the heat absorbed from the heating surface is greater than the heat delivered to heating surface the temperature decreases. The changes in time of heat flux absorbed by bubbles introduce the nonlinearity into the process of heat transfer between the heating surface and subsequent bubbles.

The correlation dimension of attractor shown in Fig. 4c is equal to 3.7 and the largest Lyapunov exponent is equal to 32 bit/s. The value the largest Lyapunov exponent corresponds to the frequency of bubbles departure. It means that the process of stability loss occurs approximately in time interval equal to average time interval of single bubble growth. Therefore we can conclude that the process of heat transfer between the heating surface and a single bubble is unstable. This lack of stability leads to deterministic chaos appearance in the temperature time series at nucleation site.

During the subsequent bubbles departure the maximum and minimum values of temperature under nucleation site depend on intensity of heating the silicon surface by laser ray and the intensity of cooling the silicon surface by bubbles. The moments for which the temperature reaches maximum or minimum values divide the time series of temperature changes into subsequent time periods. The temperature at the end of each time interval is an indicator of heat transfer within each time interval.

In Fig. 5a it has been shown the chart $T_{k+1}(T_k)$ from time series that consists of maximum and minimum values of temperature at the single nucleation site for long time series. The noise existing in the system causes that it is difficult to recognize in Fig. 5a the relations between the $T_{k+1}$ and $T_k$. In Fig. 5b it has been shown the chart $T_{k+1}(T_k)$ constructed basing on the short time series of maximum and minimum values of temperature at the single nucleation site. The result allows us to conclude that during the subsequent bubbles departures the temperature oscillates between two groups of points. In our opinion the short time series seem to be less sensitive to boundary condition changes around the nucleation site therefore the dynamic of direct interaction between the

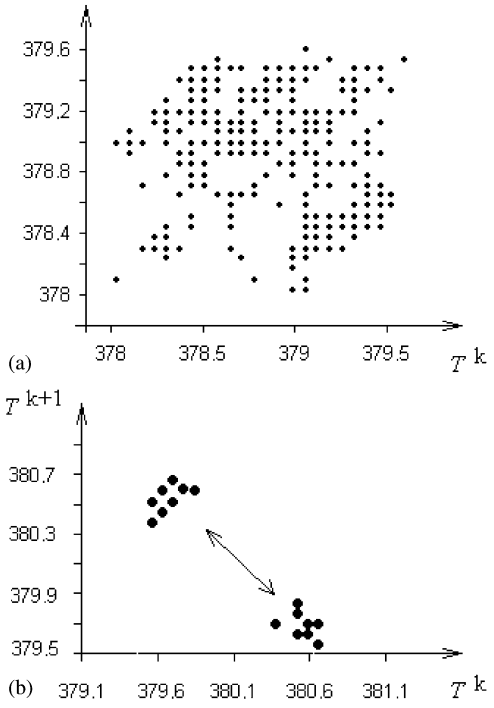


Fig. 5. The return map of maximum and minimum temperature of heating surface for $q = 34.4$ kW/m$^2$. (a) for long time series, (b) for short time series.

subsequent bubbles and heating surface can be recognized.

## 4. Nucleation sites interaction

To investigate the nucleation sites interaction, the silicon surface with twin cylindrical nucleation sites was used. The nucleation sites of 10 μm in diameter and 80 μm in depth was applied. The spacing, $S$, between two nucleation sites, was changed from 1 to 8 mm. As the size of the departing bubble without interference, $D$, was approximately 2.4 mm in diameter, the spacing employed corresponds to the spacing-to-bubble diameter ratio, $S/D$, from 0.3 to 3.3.

The existence of neighbouring nucleation site makes that the temperature changes become more complex in comparison with the temperature changes at the single nucleation site. In Fig. 6 it has been shown the example of the temperature changes at nucleation site when in its neighbourhood there is, in distance of 2 mm, another nucleation site. A black line over the $t$-axis shows the average time interval of bubble growth.

The attractor reconstruction from the temperature changes allows us to identify the nature of processes responsible for increase in the complexity of temperature changes. Fig. 7 shows the 3D attractor reconstruction from the temperature at the nucleation site for different distances between neighbouring nucleation sites. Under the single nucleation site the attractor has a triangle shape shown in Fig. 4. When the distance between the nucleation sites increases the shape of one of sections of attractor is also similar to a triangle but in the direction perpendicular to this section the shape becomes more complex. It is possible to notice this change in Fig. 7a and d.

The triangle shape of attractor and its modification is created by different kind of temperature changes. In Fig. 6 two characteristic kinds of temperature changes have been marked. In the first area marked with a number "1" the temperature changes occur with relatively less amplitude compared with temperature changes in the area "2". Because the temperature changes in area "2" occur rarelier than in the area "1" therefore the part of attractor at lower density of points is created by temperature changes shown in the area "2". This kind of modification of attractors shape occurs in attractors shown in Fig. 7a–c for $0.3 < S/D < 1.2$. But one of section of high density area of attractors (Fig. 7a–c) is still similar to a triangle like in case of single nucleation site (Fig. 4). It suggests that the character of temperature changes in the area "1" is similar to the temperature changes occurring under the single nucleation site. The existence of neighbouring nucleation site modifies the temperature time series adding the disturbance shown in area 2 in Fig. 6. This kind of disturbances increases attractor complexity.

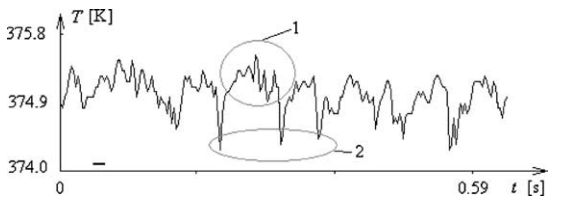


Fig. 6. Temperature changes under a nucleation site. Twin nucleation site distance equal to 2 mm, $q = 26.5$ kW/m$^2$.

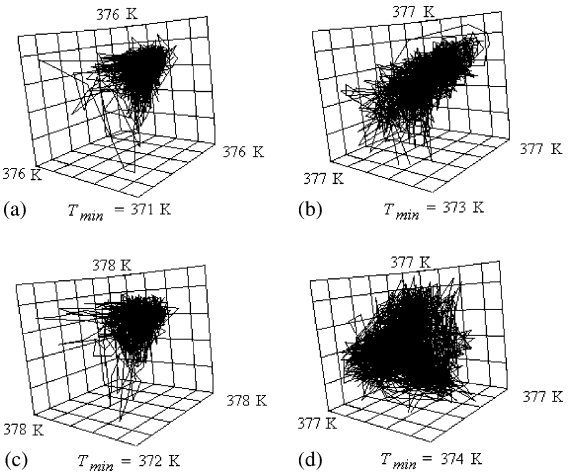


Fig. 7. 3D attractors reconstruction from the temperature fluctuation under a nucleation site, $q = 26.5$ kW/m$^2$, time delay 0.023 s. (a) Twin nucleation sites distance equal to $S/D \approx 0.3$. (b) Twin nucleation sites distance equal to $S/D \approx 0.75$. (c) Twin nucleation sites distance $S/D \approx 1.2$. (d) Twin nucleation sites distance equal to $S/D \approx 1.75$.

The dimension spectrum $D_q$ is one of the essential characteristics of attractors, it allows us to identify the structure of attractors, especially the level of complexity of attractor versus attractor points density. It is defined by the following expression [11,14,16]:

$$D_q = \lim_{l \to 0} \frac{1}{\ln d} \ln C^q(d) \tag{1}$$

where

$$C^q(d) = \left[ \frac{1}{N} \sum_i \left( \frac{1}{N} \sum_j \Theta\left(d - |X_i - X_j|\right) \right)^{q-1} \right]^{1/q-1} \tag{2}$$

$\Theta$, Heaviside's step function that determines the number of attractor's point pairs of the distance shorter than $d$; $q$, parameter.

Parameter $q$ indicates us for which density of attractor points the dimension is calculated. When $q \to -\infty$ then $D_q$ characterizes the part of attractor with

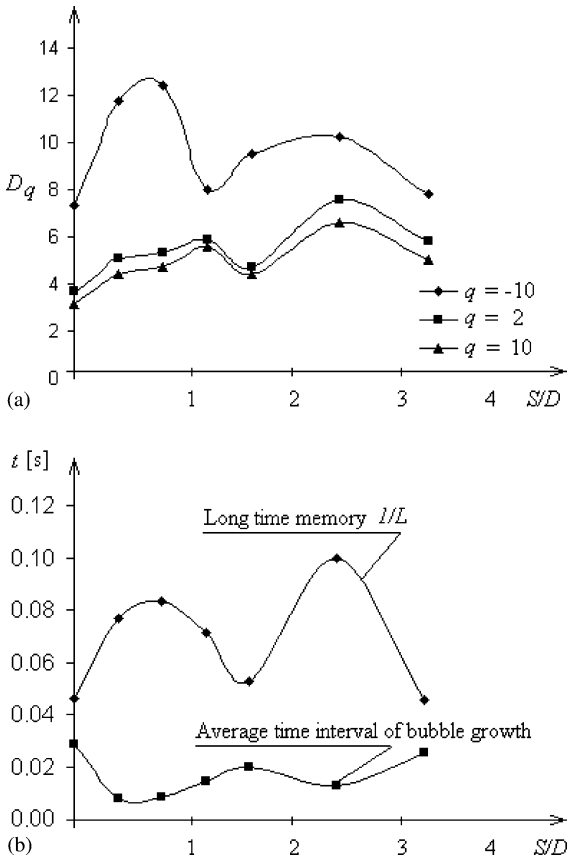


Fig. 8. Fractal analysis of temperature fluctuation. (a) $D_q$ dimension against the distance between the nucleation sites ($D_q$ was calculated according to the Grassberger and Procaccia algorithm [11]). (b) A long time memory interval and time interval of bubble growth $q = 26.5$ kW/m$^2$. The largest Lyapunov exponent was calculated according to the Wolf algorithm [12].

low density of points. When $q \to +\infty$ then dimension $D_q$ characterizes the area of attractor with high density of points. In Fig. 8a the dimensions $D_{-10}$, $D_2$, $D_{+10}$ of attractors from temperature fluctuation at one of two nucleation sites against the distance between the nucleation sites have been presented. The charts of dimensions $D_{-10}$ and $D_{10}$ against distance between nucleation sites indicate how the structure of different parts of attractor changes. A high density part of attractors characterized by dimension $D_{10}$ is created by temperature changes marked by "1" in Fig. 6. The low density part of attractors corresponds to temperature changes marked in Fig. 6 by number "2" and are characterized by dimension $D_{-10}$. In other words the dimension $D_{-10}$ characterizes the dynamic of interaction between the departing bubbles (large scale of temperature changes) and dimension $D_{10}$ characterizes the dynamic of direct heat transfer between the bubbles and heating surface (small scale of temperature changes). The correlation dimension $D_2$ characterizes the whole structure of attractors.

When the distance between the nucleation sites is not too large ($S/D < 1.5$) the bubbles interact over the heating surface as well as through horizontal heat transfer inside the heating surface.

For $0 < S/D < 1.5$ the dimension $D_{-10}$ changes more rapidly compared with the dimension $D_{10}$. Because in this area the different processes of coalescence occur then we can assume that these processes are responsible for increase of $D_{-10}$. The dimension $D_{-10}$ reaches a minimum value at $S/D \approx 1.25$ when the coalescence process disappears. The dimension $D_{10}$ reaches a minimum value at $S/D \approx 1.75$, in this case we can assume that the thermal interaction disappears.

The another important characteristic of attractor is the largest Lyapunov exponent. In this case on the attractor immersed in $D$ dimensional space two points have been selected. The distance between these two points $d(t_j)$ is at least one orbiting period. After the passage of some evolution time the distance of the selected points has been calculated again and denoted as $d(t_{j+1})$. The largest Lyapunov exponent has been calculated according to formula:

$$L = \frac{1}{t}\sum_{j=1}^{m} \log_2 \frac{d(t_{j+1})}{d(t_j)} \tag{3}$$

where $m$—number of examined points, $t$—time of evolution.

The largest Lyapunov exponent allows us to calculate time period $(1/L)$ of long time memory in the system in which the process of stability loss occurs. The comparison between the value of long time memory calculated from the largest Lyapunov exponent and the average time interval of bubble growth has been presented in Fig. 8b.

The decrease of the largest Lyapunov exponent (for $0 < S/D < 1.5$) means that the process becomes more predictable. It can be interpreted as a result of memorizing the state of one nucleation site by another one. In this process the information about the state of one nucleation site is transferred to the neighbouring nucleation site through the coalescence process and through the modification of temperature field of the heating surface. From this point of view the process of bubbles generation at close nucleation sites resembles the generation of large bubbles (created in results of bubbles coalescence) from a single nucleation area (consisting of two nucleation sites). The frequency of bubbles departure from two nucleation sites increases due to coalescence process whereas the large bubble creation time is a multiple of time of bubbles created at nucleation sites. This time of creation of large bubble (created in results of bubbles coalescence) is detected in result of analysis of largest Lyapunov exponent and shown in Fig. 8b.

For $S/D \approx 1.5$ the coalescence process disappears and the process of hydrodynamic interaction between the bubbles begins. This process is caused by liquid flow induced by departing bubbles. In this region the dimensions $D_{-10}$, $D_2$, $D_{+10}$ increase and the largest Lyapunov exponent decreases. It seems that the liquid flow induced by neighbouring bubbles changes the condition over the nucleation sites and finally it changes the dynamic of bubble growth. The changes of dynamics of bubble growth induced by liquid flow can considerably influence on complexity of dynamics of direct heat transfer between the bubbles and the heating surface. It happens due to information transfer (through liquid flow that is induced by bubbles) about the conditions at nucleation sites. The largest Lyapunov exponent decreases (process becomes more predictable) but the frequency of bubbles departure slightly increases. When $S/D$ approaches about 3 the bubbles become independent.

## 5. Modelling

For identification of mechanism of appearance of chaotic changes of temperature at nucleation site the heat transfer in a square element containing a single nucleation site has been considered. The maximum and minimum values of temperature divide the time series of temperature changes into subsequent time intervals. In the presented model these intervals are equal to each other. Data presented in Fig. 3 show that this assumption is close to experimental results. For such time intervals we can define the constant average heat flux absorbed by bubble. The average heat flux can be defined in such a way so that the temperature of heating surface at the end of each time intervals could reach the maximum or minimum value of temperature observed in experiment. The area of heating surface has been divided into the square elements shown in Fig. 9. The linear dimension of square elements was similar to average diameter (3.5 mm) of bubbles departing from a single nucleation site.

Fig. 9 depicts the element '*i*' of heating surface containing the nucleation site. During the boiling process the heat is transferred to and from element '*i*' in the subsequent time intervals $k$. The heat flux supplied to the bottom of element '*i*' has been denoted as $q_d^k$. The bubbles growing on the heating surface absorb the heat from the element '*i*'. The heat flux absorbed by bubbles from the element '*i*' has been denoted as $q_u^k$. It has been assumed that within subsequent time intervals '*k*' the values of $q_d^k$ and $q_u^k$ are constant. These values can be treated as average values of $q(t)$ in time interval $k$. It has been assumed that the value of $q_d^k$ is constant in time (in whole simulation) and the value of $q_u^k$ changes in subsequent time intervals. The direction of heat transfer

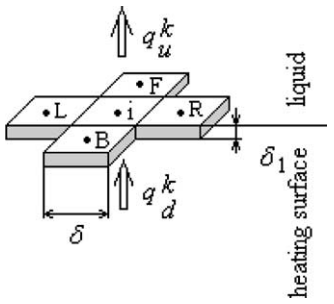


Fig. 9. Schematic drawing of the model.

between the element '*i*' and his surrounding elements depends on the temperature difference between the temperature of element '*i*' and the temperature of surrounding elements.

The heat balance equation in the element '*i*' has a form:

$$\begin{aligned} & q_d^k \cdot \delta \cdot \delta \cdot \Delta t - q_u^k\left(T_i^k\right) \cdot \delta \cdot \delta \cdot \Delta t \\ & \quad + \frac{\lambda\delta \cdot \delta_1\left(T_{\mathrm{L}} - T_i^k\right)\Delta t}{\delta} - \frac{\lambda\delta \cdot \delta_1\left(T_i^k - T_{\mathrm{R}}\right)\Delta t}{\delta} \\ & \quad + \frac{\lambda\delta \cdot \delta_1\left(T_{\mathrm{B}} - T_i^k\right)\Delta t}{\delta} - \frac{\lambda\delta \cdot \delta_1\left(T_i^k - T_{\mathrm{F}}\right)\Delta t}{\delta} \\ & \quad = \delta \cdot \delta \cdot \delta_1 \cdot \rho \cdot c \cdot \left(T_i^{k+1} - T_i^k\right) \end{aligned} \tag{4}$$

where $T_i^k$ is an average temperature of element '*i*', $q_u^k\left(T_i^k\right) \cdot \delta \cdot \delta \cdot \Delta t$ is a heat transferred from element '*i*' to liquid in time interval $\Delta t$, $q_d^k \cdot \delta \cdot \delta \cdot \Delta t$ is a heat transferred from the heating surface to the element '*i*' in time interval $\Delta t$ and $\delta \cdot \delta \cdot \delta_1 \cdot \rho \cdot c \cdot \left(T_i^{k+1} - T_i^k\right)$ is the increase of energy of element '*i*'.

After transformations of Eq. (4) it has been obtained:

$$\begin{aligned} T_i^{k+1} = T_i^k + \frac{1}{A}\Bigg[ & q_d^k \frac{\delta}{\delta_1}\frac{\delta}{\lambda} - q_u^k\left(T_i^k\right)\frac{\delta}{\delta_1}\frac{\delta}{\lambda} - 4T_i^k + T_{\mathrm{L}} \\ & + T_{\mathrm{R}} + T_{\mathrm{B}} + T_{\mathrm{F}}\Bigg] \end{aligned} \tag{5}$$

where $A = \frac{\delta^2 \cdot \rho \cdot c}{\lambda \Delta t} = \frac{1}{Fo}$.

The function (5) allows us to calculate the heat flux absorbed by bubbles when the temperature $T_i^{k+1}$ is a known function of $T_i^k$. After the transformation of Eq. (5) it has been obtained:

$$\begin{aligned} q_u^k\left(T_i^k\right) = \frac{\lambda}{\delta}\Bigg\{ & q_d^k \frac{\delta}{\delta_1}\frac{\delta}{\lambda} - 4T_i^k + T_{\mathrm{L}} + T_{\mathrm{R}} + T_{\mathrm{B}} + T_{\mathrm{F}} \\ & + A \cdot T_i^k - A \cdot T_i^{k+1}\Bigg\} \Bigg/ \frac{\delta}{\delta_1} \end{aligned} \tag{6}$$

When $q_d^k$ is constant in time and $q_u^k$ is a linear function of $T_i^k$ in two subsequent time intervals then the function $T_i^{k+1} = f\left(T_i^k\right)$ (Eq. 5) can be written in the form:

$$T_i^{k+1} = \begin{cases} a_1 T_i^k + b_1 & \text{for } T_i^k < T_c \\ a_2 T_i^k + b_2 & \text{for } T_i^k \geqslant T_c \end{cases} \quad (7)$$

where $T_c$ is a crossing point of lines described by Eq. (7).

The function (7) consists of two crossing lines. The behavior of such system described by set of Eq. (7) for $|a_1| > 1$ can become chaotic [13]. In the paper [13] it has been shown that when the heat transfer to thin layer of heating surface is enough large then the initial fluctuation of temperature disappear and the temperature stabilizes. But when the heat transfer to thin layer of heating surface is less than heat absorbed by bubbles then the initial fluctuation of temperature is amplified and deterministic chaos appears.

The values of coefficients $a$ and $b$ have been taken is such a way that subsequent iterations of temperature $T_i^k$ described by equation (7) are close to experimental data. In Fig. 10a it has been shown the comparison of experimental data and subsequent iterations of Eq. (7).

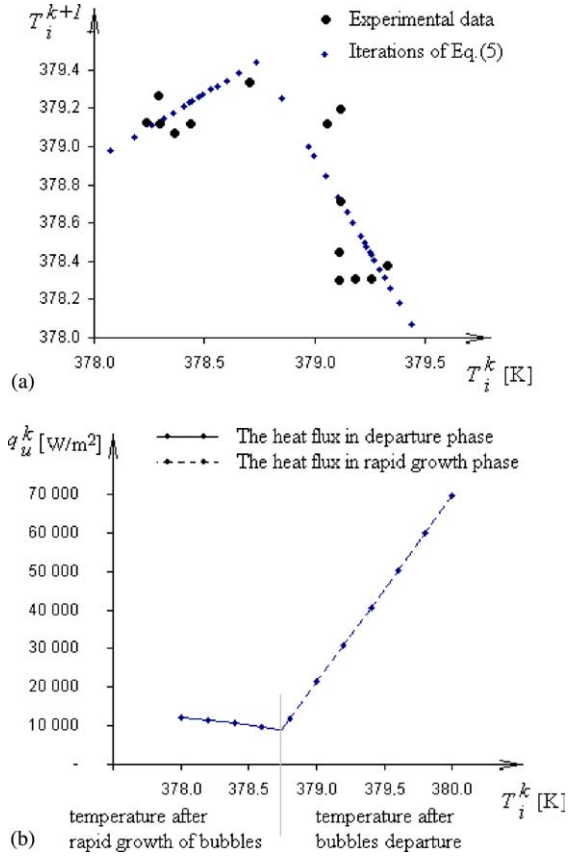


Fig. 10. Changes of $T_i^{k+1}$ and $T_i^k$. (a) function of $T_i^{k+1}(T_i^k)$—according to the Eq. (5), (b) function of $q_u^k(T_i^k)$—according to the Eq. (3), Calculation has been made for: $a_1 = 0.7$, $a_2 = -2$, $b_1 = 114.32$, $b_2 = 1136.95$, $T_c = 378.75$ K, $T_L = T_R = T_F = T_B = 378$ K and $\lambda = 148.4$ W/mK (silicon), $\delta = 0.0035$ m, $\delta_1 = 0.0002$ m, $Fo = 1/8$, $q_d^k = 30$ kW/m$^2$.

Fig. 10b shows the function of $q_u^k$ against $T_i^k$. The value of $Fo = 1/8$ used in calculation corresponds to $\Delta t \approx 0.017$ s. The time period of single bubble growth is equal to $2\Delta t$. In this case the frequency of bubbles departure is equal to 30 Hz and is close to frequency of single bubble departure obtained in the experiment [18].

The temperature $T_c$ in Eq. (7) may be treated as the temperature which divides the bubble growth into two phases: a rapid growth of a bubble and departure phase which is shown in Fig. 10b.

From theoretical point of view the Eq. (7) may be replaced by another function, for example quadratic function of $T^k$. This problem was discussed in details in the paper [13]. The obtained result can be considered in the following way: the nonlinearity introduced to heat transfer process by changing in time the heat flux absorbed by bubbles leads to chaotic changes of heating surface temperature at nucleation site.

The presented model can be also used to simulate the behavior of bubbles interaction through the horizontal heat transfer between neighbouring nucleation sites. For this purpose the area consisting of 25 squares has been analysed. On such a surface two nucleation sites have been located. The simulation has been made for the square silicon heating surface of side of square equal to 3.5 mm and thickness equal to 0.2 mm.

The correlation between two time series of temperature changes at nucleation sites can be estimated by using the correlation coefficient calculated according to the following formula [17]:

$$C_{i,j} = \frac{\mathrm{Cov}(T_i, T_j)}{\sigma_{T_i}\sigma_{T_j}} \quad (8)$$

The result of calculation of correlation coefficient of two time series of temperature at neighbouring nucleation sites has been shown in Fig. 11.

At the beginning of the simulation the initial conditions in both nucleation sites are the same. It causes that at the beginning of the simulation the both temperature time series are the same. After some time two temperature time series start to differ. When the distance between the nucleation sites becomes smaller then the time, in which the difference between two time series appears, becomes shorter. In this case the correlation coefficient decreases, it happens because nucleation sites interact through horizontal heat transfer. For $S/D > 2$ the thermal interaction between the nucleation sites disappears. In this case the time period, after which the difference between two time series occurs, increases. This effect of disappearance of thermal interaction between nucleation sites for $S/D \approx 2$ has been also observed in the experiment.

The obtained results can be considered in the following way: the thermal interaction of chaotic nucleation sites leads to independency of the nucleation sites.

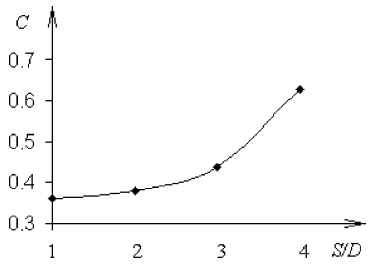


Fig. 11. The correlation coefficient for time series of the temperature under the neighbouring nucleation sites. Calculation has been made for: $a_1 = 0.7$, $a_2 = -2$, $b_1 = 114.32$, $b_2 = 1136.95$, $T_c = 378.75$ K, $\lambda = 148.4$ W/mK (silicon), $\delta = 0.0035$ m, $\delta_1 = 0.0002$ m, $Fo = 1/8$, $q_d^k = 60$ kW/m$^2$.

Other words we can say that the interacting chaotic nucleation sites cannot synchronize in a result of horizontal heat transfer inside the heating surface.

If we assume that there are many nucleation sites on the heating surface the model can be used to simulate the process of boiling on the flat and horizontal heating surface. Fig. 12 illustrates the changes of location of bubbles over 25 potential nucleation sites. The bubbles are denoted by black squares. The numbers indicate the numbers of iterations (numbers of cycles of bubble departures). At the beginning of simulation all the bubbles are in nucleation sites but after about 100 iterations the locations of bubbles due to thermal interaction become chaotic.

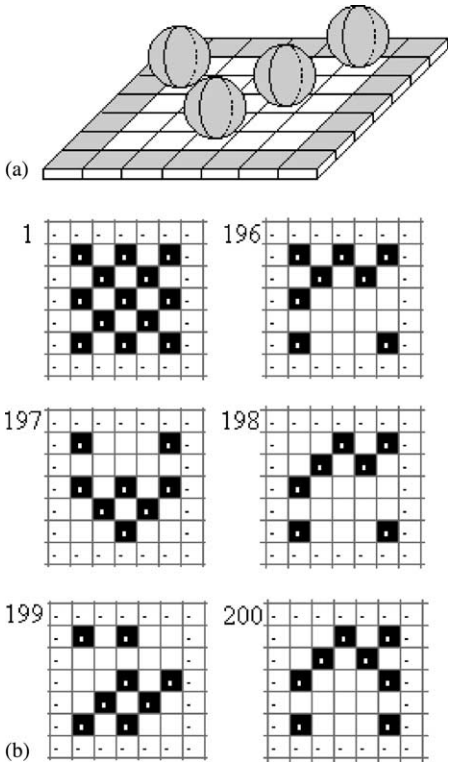


Fig. 12. Boiling modelling. (a) Schematic drawing of heating surface with many potential nucleation sites. (b) The changes of location of bubbles over 25 potential nucleation sites. The bubbles are denoted by black squares. The numbers under the pictures indicate the numbers of iterations. $q = 60,000$ kW/m$^2$.

The chaotic appearance of the bubbles at the nucleation sites after some iteration takes place because the thermal interaction between the nucleation sites occurring inside the heating surface leads to independency of nucleation sites. Nonlinear analysis carried out in the previous chapter suggests that the synchronization of nucleation sites can appear in a result of hydrodynamic interaction which can lead to forming the vapour film on the heating surface. This mechanism is not included in the model.

## 6. Conclusions

Analysis of temperature fluctuation under the single nucleation site has shown the deterministic chaos nature of this fluctuation. The simple model of heat transfer between the bubbles and heating surface, presented in the paper, explains the mechanism of chaos generation in boiling. It has been found that this mechanism is connected with nonlinearity introduced to heat transfer process by changing in time the heat flux absorbed by bubbles.

The analyses of behavior of nucleation sites interaction allow us to conclude that the effect of interaction (information transfer) between nucleation sites through the liquid (coalescence and hydrodynamic interaction) promotes the growing bubble to depart. It happens for $S/D \approx 0.5$ and 2.5. Nonlinear analysis shows that in this case the system becomes more predictable. When the nucleation sites become independent then the frequency of bubble departure decreases. Simulation of thermal interaction between the nucleation sites shows that this kind of interaction of chaotic nucleation sites leads to getting independency of the nucleation sites. Finally the frequency of bubble departure decreases and system becomes less predictable. It happens for $S/D \approx 1.75$.

We can conclude that the nonlinear analyses carried out in the paper allow us to distinguish two mechanisms of interaction between neighbouring nucleation sites: hydrodynamic one occurring over the heating surface and thermal one occurring inside the heating surface. Generally we can say that interaction between the nucleation sites through the liquid stabilizes the process of bubble growth and departure. The thermal interaction destabilizes the process of bubble growth and departure.

## Acknowledgements

The authors would like to express their appreciation to Dr. Lei Zhang for her continuous discussion and contribution in performing the experiment.

## References

[1] R.L. Judd, On nucleation site interaction, J. Heat Transfer 110 (1988) 475–478.
[2] D.M. Qiu, V.K. Dhir, Single bubble dynamics during nucleate boiling under low gravity conditions, in: Engineering Foundation Conference on Microgravity Fluid Physics and Heat Transfer, Hawaii, 1999, pp. 61–71.
[3] V.V. Chekanov, Interaction of centers in nucleate boiling, Teplofiz. Vys. Temp. 15 (1977) 121–128.
[4] A. Calka, R.L. Judd, Some aspects of the interaction among nucleation sites during saturated nucleate boiling, Int. J. Heat Mass Transfer 28 (1985) 2331–2342.
[5] H. Gjerkeš, I. Golobic, Measurement of certain parameters influencing activity of nucleation sites in pool boiling, Exp. Therm. Fluid Sci. 25 (2002) 487–493.
[6] H. Kubo, H. Takamatsu, H. Honda, Effects of size and number density of micro-reentrant cavities on boiling heat transfer from a Silicon chip immersed in degassed and gas-dissolved FC-72, Enhanced Heat Transfer 6 (1999) 151–160.
[7] S.H. Bhavnani, G. Fournelle, R.C. Jaeger, Immersion-cooled heat sinks for electronics: insight form high-speed photography, IEEE Trans. Comp. Packag. Technol. 23 (2001) 166–176.
[8] L. Zhang, M. Shoji, Nucleation site interaction in pool boiling on the artificial surface, Int. J. Heat Mass Transfer 46 (2003) 513–522.
[9] Y. Takagi, M. Shoji, Boiling features from a single artificial cavity, Int. J. Heat Mass Transfer 44 (2001) 2763–2776.
[10] J.H. Ellepola, D.B.R. Kenning, Nucleation site interactions in pool boiling. in: Second European Thermal-Sciences and 14th UIT National Heat Transfer Conference. 1996, pp. 1669–1675.
[11] P. Grassberger, I. Procaccia, Measuring the strangeness of strange attractors, Physica D 9 (1985) 189–208.
[12] A. Wolf, J.B. Swift, H.L. Swinney, J.A. Vastano, Determining lyapunov exponent from a time series, Physica D 16 (1985) 285–317.
[13] R. Mosdorf, The mechanism of generation of chaotic fluctuation of heating surface temperature in nucleate boiling, Trans. Inst. Fluid-Flow Mach. 111 (2002) 1–17.
[14] H.G. Schuster, Deterministic chaos an introduction, Physik-Verlag GmbH, Weinheim, 1984.
[15] D.B.R. Kenning, Youyou Yan, Pool boiling heat transfer on a thin plate: features revealed by liquid crystal thermography, Int. J. Heat Mass Transfer 39 (15) (1996) 3117–3139.
[16] K. Pawelzik, H. Schouster, Generalized dimension and entropies from a measured time series, Phys. Rev. A (Rapid Commun.) 35 (1) (1987) 481–483.
[17] L. Gajek, M. Kaluszka, Wnioskowanie statystyczne modele i metody, WNT, Warsaw, 2000 (in Polish).
[18] M. Shoji, R. Mosdorf, L. Zhang, Y. Takagi, K. Yasui, M. Yokota, Features of boiling on an artificial surface—bubble formation, wall temperature fluctuation and nucleation site interaction, in: First International Symposium on Thermal Science and Engineering, Beijing, China, October 23–26, 2002, pp. G293–302.